

Berry Phase, Atom Interferometry, and Observation of the Gravitational Aharonov-Bohm Effect

Huan Q. Bui*

MIT-Harvard Center for Ultracold Atoms, Research Laboratory of Electronics, and Department of Physics,
Massachusetts Institute of Technology, Cambridge, Massachusetts 02139, USA

(Dated: May 7, 2022)

Following the conception of the Aharonov-Bohm effect due to Ehrenberg, Siday, Aharonov, and Bohm in the mid-20th century, experimental verifications of the effect emerged in the late 1980s and opened up developments in matter-wave interferometry. Starting in the 1990s, interests in atom interferometry grew as physicists realized the atom's remarkable ability as a quantum sensor. In this paper, we review the notion of Berry phase and interpret the Aharonov-Bohm effect as an example. Then, we review the principles of atom interferometry, specifically two atom-light interactions which are instrumental to modern atom interferometers. Finally, we briefly survey and contextualize the recent observation of the gravitational analog of the Aharonov-Bohm effect due to Overstreet *et al.*

I. INTRODUCTION

The outline of this paper is as follows. Section II is a review of the Berry phase and the Aharonov-Bohm effect. While these topics are standard subjects of many quantum mechanics textbooks (see, for example, [1], [2], [3]), there is a wide variability in the style and context in which they are presented. The author therefore believes it is beneficial to provide a self-contained exposition here, to have the theory right at our fingertips. Section III reviews the principles of atom interferometry, with an emphasis on two atom-light interactions that are crucial for modern atom interferometers: stimulated Raman transitions and Bragg diffraction. Section IV is a brief review of the recent observation of a gravitational analog of the Aharonov-Bohm effect due to Overstreet *et al.* [4].

II. BERRY PHASE

Consider $\mathcal{H}(\mathbf{R}(t))$, a time-dependent Hamiltonian parameterized by a family of variables $\mathbf{R}(t)$. Let $|\psi(0)\rangle = |n(\mathbf{R}(0))\rangle$ where $|n(\mathbf{R}(0))\rangle$ is the n^{th} eigenstate of $\mathcal{H}(\mathbf{R}(0))$. By the adiabatic theorem, $|\psi(t)\rangle$ is $|n(\mathbf{R}(t))\rangle$, the n^{th} instantaneous eigenstate of $\mathcal{H}(t)$, up to a phase factor, i.e.,

$$|\psi(t)\rangle = e^{-\frac{i}{\hbar} \int_0^t E_n(\mathbf{R}(t')) dt'} \exp(i\gamma_n(t)) |n(\mathbf{R}(t))\rangle,$$

where $\gamma_n(t)$ is called the *Berry phase*. Since $|\psi(t)\rangle$ solves the Schrödinger equation $\mathcal{H}(\mathbf{R}(t))|\psi(t)\rangle = i\hbar(d/dt)|\psi(t)\rangle$, we have

$$\dot{\gamma}_n(t) = i \langle n(\mathbf{R}(t)) | \nabla_{\mathbf{R}} | n(\mathbf{R}(t)) \rangle \cdot \dot{\mathbf{R}}(t).$$

In particular, at some final time t_f ,

$$\gamma_n(t_f) = \int_{\mathbf{R}_i}^{\mathbf{R}_f} i \langle n(\mathbf{R}) | \nabla_{\mathbf{R}} | n(\mathbf{R}) \rangle \cdot d\mathbf{R}, \quad (1)$$

which depends only on the path in parameter space over which the evolution takes place. Define the *Berry connection*,

$$\mathbf{A}_n(\mathbf{R}) = i \langle n(\mathbf{R}) | \nabla_{\mathbf{R}} | n(\mathbf{R}) \rangle$$

and consider gauge transformation in parameter phase of instantaneous eigenstates $|n(\mathbf{R})\rangle \rightarrow |\tilde{n}(\mathbf{R})\rangle = e^{-i\beta(\mathbf{R})} |n(\mathbf{R})\rangle$. The Berry connection transforms like the electromagnetic vector potential:

$$\mathbf{A}_n(\mathbf{R}) \rightarrow \widetilde{\mathbf{A}}_n(\mathbf{R}) = \mathbf{A}_n(\mathbf{R}) + \nabla_{\mathbf{R}}\beta(\mathbf{R}),$$

while the Berry phase transforms as

$$\widetilde{\gamma}_n(\mathbf{R}) = \int_{\mathbf{R}_i}^{\mathbf{R}_f} \widetilde{\mathbf{A}}_n(\mathbf{R}) \cdot d\mathbf{R} = \gamma_n(\mathbf{R}_f) + \beta(\mathbf{R}_f) - \beta(\mathbf{R}_i)$$

which is gauge-invariant exactly when the Hamiltonian evolution is cyclical, i.e., $\mathbf{R}(t_f) = \mathbf{R}(0)$. In such a case, the Berry phase is well-defined and measurable by means of interferometry.¹

A. Aharonov-Bohm Effect

The Aharonov-Bohm effect is often discussed in the context of the path integral formulation of quantum mechanics where one compares the wavefunctions for a charged particle passing along two (distinct) paths in a vector potential \mathbf{A} associated with some magnetic field

* huanbui@mit.edu

¹ There is also the notion of the *Berry curvature*, but it is not relevant to the scope of this paper.

B. Here, the author presents M. V. Berry's interpretation of the Aharonov-Bohm effect as a Berry phase change. This is not only an illustrative application of (1), but also avoids issues with single-valuedness of wavefunctions that arise in [5] and [6] as suggested by Berry.

Consider a particle of mass m and charge q in a magnetic field \mathbf{B} generated by a thin long solenoid. For positions \mathbf{R} outside the solenoid and enclosing it by a closed path C , the magnetic field is zero but the circulation of the vector potential \mathbf{A} along C is the total magnetic flux:

$$\oint_C \mathbf{A}(\mathbf{R}) \cdot d\mathbf{R} = \Phi_B.$$

Let the particles be confined to a box at \mathbf{R} . The particle Hamiltonian depends on position \mathbf{r} and conjugate momentum \mathbf{p} as $\mathcal{H} = \mathcal{H}(\mathbf{p}, \mathbf{r} - \mathbf{R})$ when $\mathbf{A} = 0$. Let the wavefunctions be $\psi_n(\mathbf{r} - \mathbf{R})$ with eigenvalues E_n . When $\mathbf{A} \neq 0$, the Hamiltonian satisfies

$$\mathcal{H}(\mathbf{p} - q\mathbf{A}(\mathbf{R}), \mathbf{r} - \mathbf{R}) |n(\mathbf{R})\rangle = E_n |n(\mathbf{R})\rangle$$

since the vector potential does not affect the energies. The solutions for this Hamiltonian have the form

$$\langle \mathbf{r} | n(\mathbf{R}) \rangle = \exp \left[\frac{iq}{\hbar} \int_{\mathbf{R}}^{\mathbf{r}} d\mathbf{r}' \cdot \mathbf{A}(\mathbf{r}') \right] \psi_n(\mathbf{r} - \mathbf{R}).$$

We can calculate the total phase change after transporting the box around C starting with

$$\begin{aligned} & \langle n(\mathbf{R}) | \nabla_{\mathbf{R}} | n(\mathbf{R}) \rangle \\ &= \int d^3\mathbf{r} \psi_n^*(\mathbf{r} - \mathbf{R}) \left[\frac{-iq}{\hbar} \psi_n(\mathbf{r} - \mathbf{R}) + \nabla_{\mathbf{R}} \psi_n(\mathbf{r} - \mathbf{R}) \right] \\ &= -\frac{iq\mathbf{A}(\mathbf{R})}{\hbar}. \end{aligned}$$

From here,

$$\gamma_n(C) = \frac{q}{\hbar} \oint_C \mathbf{A}(\mathbf{R}) \cdot d\mathbf{R} = \frac{q\Phi_B}{\hbar},$$

which is independent of both n and C , so long as C encloses the solenoid once.

III. ATOM INTERFEROMETRY

It is clear from the theoretical description of the (classically inconceivable) Aharonov-Bohm effect that in order to observe it, the experimenter must allow matter to interfere. “Interferometers” often refer to *optical interferometers* where light waves from a single source travel different paths and interfere constructively or destructively when recombined depending on the relative phase they have accumulated along their paths. The interference pattern allows one to extract information about difference in the path length. Some well-known optical interferometers include the Michelson interferometer

and the Laser Interferometer Gravitational-Wave Observatory (LIGO)².

Matter-wave interferometers work based on similar principles, but rely on the wave-like nature of particles. Following the first³ observation of the magnetic Aharonov-Bohm effect in the late 1980s using electron matter-waves [7], new developments in atomic, molecular, and optical physics led to interferometry using neutral atoms (some early examples include [12] and [13]). Atom interferometry are well-suited for precision measurements, gravitational wave sensors, and tests of tests of relativity due to their short de Broglie wavelengths compared to their optical counterpart as well as having nonzero mass, which allows them to interact with gravity [14], [15], [16]. Moreover, atoms possess high controllability thanks to their internal structure and lack electric charge, making them insensitive to undesired environmental influences such as stray electric or magnetic fields [17].

While early atom interferometers such as that developed by [12] used slits and wires to split and reflect atoms, modern iterations manipulate atoms using light forces [18]. These are thus called *light-pulse atom interferometers* [19]. They generically works as follows: when light resonantly interacts with an atom, Rabi oscillations occur. A $\pi/2$ pulse puts a two-level atom in a 50:50 superposition of the ground and excited state and therefore act as a beamsplitter, while a π pulse inverts the population of the ground and excited states, acting as a mirror. Atoms are deflected by light because of the photon momentum: The light pulses correlate the internal states of an atom to its momentum states. For example, an atom in its ground state $|g\rangle$ with momentum \mathbf{p} ($|g, \mathbf{p}\rangle$) is coupled to an excited state $|e\rangle$ with momentum $\mathbf{p} + \hbar\mathbf{k}$ ($|e, \mathbf{p} + \hbar\mathbf{k}\rangle$).

In the upcoming subsections, some basic principles of atom interferometry are outlined. Subsections III A describes the Mach-Zehnder atom interferometer. Subsections III B and III C present the theory of stimulated Raman transitions and Bragg diffraction, two main mechanisms for splitting and reflecting atoms using laser light in modern atom interferometers.

A. Mach-Zehnder (MZ) atom interferometer⁴

In an optical MZ interferometer, a light beam is split by a beamsplitter into two beams which travel differ-

² LIGO is a Michelson interferometer with additional components such as Fabry-Pérot cavities.

³ [7] is the first *undisputed* observation of the Aharonov-Bohm effect, where superconductors were used to shield electron waves from leakage magnetic fields. Previous observations due to [8], [9] and others in the early 1960s might have suffered from leakage fields, as suggested by [10] and [11].

⁴ The Ramsey-Bordé configuration is also standard in atom interferometry. See [14].

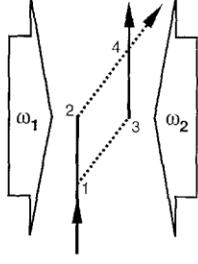


FIG. 1. Lines show the mean paths of an atom in an MZ atom interferometer. The solid (dash) lines correspond to the ground (excited) state of the atom. From [19].

ent paths and are then redirected towards each other by mirrors and recombined by a beamsplitter, making the beams interfere. Similarly, in an MZ atom interferometer (see Figure 1), a $\pi/2 - \pi - \pi/2$ pulse sequence is used to coherently split, reflect, and recombine an atomic wavepacket. The initial $\pi/2$ puts $|g, \mathbf{p}\rangle$ into $|g, \mathbf{p}\rangle + |e, \mathbf{p} + \hbar \mathbf{k}\rangle$, corresponding to two wavepackets. While $|e\rangle$ is stable against spontaneous decay to $|g\rangle$, the two wavepackets drift apart by a distance $\hbar k T/m$ over a duration T . The π pulse then inverts the population: $|e, \mathbf{p} + \hbar \mathbf{k}\rangle \rightarrow |g, \mathbf{p}\rangle$ and $|g, \mathbf{p}\rangle \rightarrow |e, \mathbf{p} + \hbar \mathbf{k}\rangle$, and the wavepackets overlap after another interval T . The second $\pi/2$ pulse “recombines” the wavepackets and causes them to interfere.[19].

As is the case in optical interferometry where longer arm lengths increase the instrument’s sensitivity, in atom interferometry the larger the wavepacket separation $\hbar k T/m$ the better. However, there is a trade-off between drift time and recoil velocities. Drift times on the order of 1s generally require metastable atomic transitions. While hyperfine transitions fulfill this requirement, the recoil velocities are small ($\sim 0.1 \mu\text{m}$ for the Na $F = 1, 3S_{1/2} \rightarrow F = 2, 3S_{1/2}$). Conversely, metastable optical transitions have large recoil velocities, but often need ultra-stable lasers to drive. The forthcoming subsections III B and III C describe two methods for obtaining large wavepacket separations in atom interferometers.

B. Stimulated Raman Transitions

Stimulated Raman Transitions is one of the first techniques developed for obtaining large recoil kicks while simultaneously meeting the metastability criterion. The following treatment⁵ of the theory follows from [19]. The Hamiltonian for the three-level system is

$$\mathcal{H} = \frac{\vec{p}^2}{2m} + \hbar\omega_1^A |1\rangle\langle 1| + \hbar\omega_2^A |2\rangle\langle 2| + \hbar\omega_i^A |i\rangle\langle i| - e\vec{r} \cdot \vec{E}$$

where $\vec{E} = \vec{E}_1 \cos(k_1 x - \omega_1 t + \Phi_1) + \vec{E}_2 \cos(k_2 x - \omega_2 t + \Phi_2)$. Here, $\omega_1, \omega_2 \sim \omega_i^A - \omega_1^A$, and $\omega_1 - \omega_2 \sim \omega_2^A - \omega_1^A$ (see Figure 2). For counter-propagating beams, $k_1 \sim -k_2$. We look for solutions to the Schrödinger equation of the form

$$|\Psi\rangle = \int dp \sum_{\alpha} a_{\alpha,p}(t) e^{-i(\omega_{\alpha}^A + p^2/2m)t} |\alpha, p\rangle$$

where $|\alpha, p\rangle$ denotes an atom in internal state $|\alpha\rangle$ and momentum eigenstate $\phi_p(x) \sim e^{ipx/\hbar}$. For a given p , the Schrödinger equation after the rotating wave approximation reduces to

$$\begin{aligned} \dot{a}_{1,p} &= \frac{i}{2} e^{i\Delta_1 t} \Omega_{1i}^* a_{i,p+\hbar k_1} \\ \dot{a}_{i,p+\hbar k_1} &= \frac{i}{2} [\Omega_{i1} e^{-i\Delta_1 t} a_{1,p} + \Omega_{i2} e^{-i\Delta_2 t} a_{2,p+\hbar k_1-\hbar k_2}] \\ \dot{a}_{2,p+\hbar k_1-\hbar k_2} &= \frac{i}{2} e^{i\Delta_2 t} \Omega_{1i}^* a_{i,p+\hbar k_1}, \end{aligned}$$

where we have assumed that the electric field \vec{E}_j only couples to the $|j\rangle \rightarrow |i\rangle$ transitions and

$$\begin{aligned} \Omega_{ji} &= e \langle i | \vec{r} \cdot \vec{E}_j | j \rangle e^{i\Phi_j/\hbar} \\ \Delta_j &= (\omega_j^A + \omega_j - \omega_i^A) + p_j^2/2m - p_i^2/2m \end{aligned}$$

with $j = 1, 2$ and i denotes the intermediate state. Adiabatic elimination⁶ of $|i\rangle$ and setting $p_1 = p, p_j = p_1 + \hbar k_1, p_2 = p + \hbar k_1 - \hbar k_2$, we obtain

$$\dot{a}_{1,p_1} \approx -\frac{i}{2} \Omega_1^{\text{AC}} a_{1,p_1} - \frac{i}{2} e^{i\delta_{12}t} \Omega_{\text{eff}} a_{2,p_2} \quad (2)$$

$$\dot{a}_{2,p_2} \approx -\frac{i}{2} \Omega_2^{\text{AC}} a_{2,p_2} - \frac{i}{2} e^{-i\delta_{12}t} \Omega_{\text{eff}}^* a_{1,p_1}. \quad (3)$$

where

$$\begin{aligned} \Omega_{\text{eff}} &= \Omega_{1i}^* \Omega_{i2} / 2\Delta, \quad \Omega_j^{\text{AC}} = |\Omega_{ji}|^2 / 2\Delta, \quad \text{and} \\ \delta_{12} &= (\omega_1 - \omega_2) - (\omega_2^A - \omega_1^A) \\ &\quad - \left[v_x(k_1 - k_2) + \frac{\hbar(k_1 - k_2)^2}{m} \right]. \end{aligned}$$

Here v_x is the velocity of the atoms along the beams. The first terms on the right of (2) and (3) lead to AC Stark shifts in $|1\rangle$ and $|2\rangle$. The second terms lead to Rabi flopping between the two levels. The effective detuning δ_{12} from the Raman resonance contains the AC Stark shifts, Doppler shifts, and recoil shifts. A resonant process transfers an atom initially in $|1, \mathbf{p}\rangle$ to $|2, \mathbf{p} + \hbar \mathbf{k}_1 - \hbar \mathbf{k}_2\rangle$. Figure 2 shows the relevant parameters for this process.

⁵ Coincidentally, Pset#12 of 8.421, Spring 2022, also treats this problem, but in a slightly different approach.

⁶ Adiabatic elimination is a tool in quantum optics often used to extract effective two-level dynamics from a three-level system driven by off-resonant light. See [20].

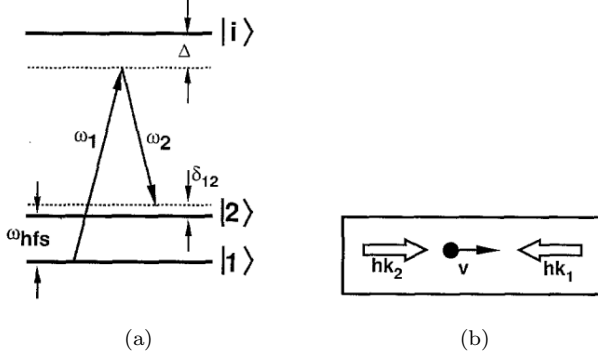


FIG. 2. (a) Energy diagram for stimulated Raman transitions between $|1\rangle$ and $|2\rangle$. Raman beams are detuned by Δ from the transitions to $|i\rangle$. δ_{12} is velocity-dependent. Following $|1\rangle \rightarrow |2\rangle$, the atom's momentum changes by $\hbar\mathbf{k}_1 - \hbar\mathbf{k}_2$. (b) Geometry for the velocity-selective configuration. From [19].

C. Bragg Diffraction

Bragg diffraction, partially invented and developed by the Holger Müller group at UC Berkeley, is another tool for generating (large) momentum transfers for atom interferometry. It may be viewed as an improvement over the two-photon stimulated Raman process since an atom generally absorbs the momentum of more than two photons while remaining in its electronic ground state. The following treatment of Bragg diffraction follows from [21]. Let ω_0 the transition frequency, $|g\rangle$ the ground state, and $|e\rangle$ the excited state and $\Omega \equiv \vec{d}_{ge} \cdot \vec{E}_0/\hbar$ be the Rabi frequency, where \vec{d}_{ge} is the dipole moment matrix element of the atom. Consider the interaction between the atom and an electric field of the form $\vec{E} = \vec{E}_0(e^{ikz - i\omega_L t} + e^{-ikz + i\omega_L t})/2$. In the near-resonance limit where $\Delta \equiv \omega_L - \omega_0 \ll \omega_0$, we may make the rotating wave approximation to obtain

$$\mathcal{H} = \underbrace{\frac{\vec{p}^2}{2m} + \hbar\omega_0 |e\rangle\langle e|}_{\equiv \mathcal{H}_0} - \left(\frac{\hbar\Omega}{2} e^{ikz - i\omega_L t} |e\rangle\langle g| + h.c. \right).$$

For generalized electric fields, $\vec{E} = \sum_j \vec{E}_j \cos(k_j z - (\omega_L - \delta_j)t)$, a generalized rotating wave approximation gives

$$\mathcal{H} \approx \mathcal{H}_0 - \left(\sum_j \frac{\hbar\Omega_j}{2} e^{ik_j z - i(\omega_L - \delta_j)t} |e\rangle\langle g| + h.c. \right)$$

where $|\delta_j| \ll \omega_L$ are small detunings from the “main” frequency ω_L and $\Omega_j \equiv \vec{d}_{ge} \cdot \vec{E}_j/\hbar$. Going back to the

rotating frame, the Hamiltonian is

$$\mathcal{H}^{\text{rot}} = \frac{\vec{p}^2}{2m} - \hbar\Delta |e\rangle\langle e| - \left(\sum_j \frac{\hbar\Omega_j}{2} e^{ik_j z + i\delta_j t} |e\rangle\langle g| + h.c. \right).$$

In Bragg diffraction, the electric field is a nearly-standing wave. After the rotating wave approximation,

$$\vec{E} \rightarrow \frac{\vec{E}_0}{2} u(z, t) = \frac{\vec{E}_0}{2} [e^{-ikz + i\delta t} + e^{ikz - i\delta t}], \quad (4)$$

where k is the laser wavevector, 2δ is the detuning between the counter-propagating beams. With this,

$$\mathcal{H}^{\text{rot}} = \frac{\vec{p}^2}{2m} - \hbar\Delta |e\rangle\langle e| - \left(\frac{\hbar\Omega u(z, t)}{2} |e\rangle\langle g| + h.c. \right).$$

The solutions to this Hamiltonian have the form

$$|\Psi\rangle = e(z, t) |e\rangle + g(z, t) |g\rangle.$$

Plugging this ansatz into the Schrödinger equation with \mathcal{H}^{rot} we find

$$i\hbar\dot{e}(z, t) = \frac{\vec{p}^2}{2m} e(z, t) - \hbar\Delta e(z, t) - \frac{\hbar\Omega}{2} u g(z, t) \quad (5)$$

$$i\hbar\dot{g}(z, t) = \frac{\vec{p}^2}{2m} g(z, t) - \frac{\hbar\Omega^*}{2} u^* e(z, t). \quad (6)$$

Since $\Delta \gg \Omega$, we may set $\dot{e}(z, t) = 0$ by adiabatic elimination. Moreover, $\Delta \gg \omega_r = \hbar k^2/2m$, the recoil frequency, and so $\vec{p}^2/2m \ll \hbar\Delta$ in (5). Solving for $e(z, t)$ and substituting into (6) gives

$$i\dot{g}(z, t) = -\frac{\hbar}{2m} \partial_z^2 g(z, t) + \frac{|\Omega|^2}{4\Delta} u u^* g(z, t). \quad (7)$$

Since the electric field $\sim u(z, t)$ is periodic, we may choose the following ansatz for $g(z, t)$ ⁷:

$$g(z, t) = \sum_{n=-\infty}^{\infty} g_n(t) e^{i2nkz} e^{-i(2n)^2\omega_r t}. \quad (8)$$

Inserting this ansatz into (7) and simplifying⁸ gives

$$i\dot{g}_n = \frac{\bar{\Omega}}{2} g_{n+1} e^{i2\delta t} e^{-i4(2n+1)\omega_r t} + \frac{\bar{\Omega}}{2} g_{n-1} e^{-i2\delta t} e^{i4(2n-1)\omega_r t} \quad (9)$$

where $\bar{\Omega} = |\Omega|^2/2\Delta$ is the two-photon Rabi frequency. This is an infinite set of coupled differential equations

⁷ This is equivalent to the ansatz in III B.

⁸ See [21] for details regarding this step.

where the plane wave momentum states of the atom are coupled only by integer multiples of the photon wavevector k . An atom starting in g_{n_I} with momentum $2n_I\hbar k$ can only be transferred to g_{n_F} with momentum $2n_F\hbar k$. The Bragg resonance condition for this process is $\delta = 2(n_F + n_I)\omega_r$.

Consider a system where an atom initially in a pure momentum state $g_{n_I} = 1$ is resonantly transferred to a state g_{n_F} via $\delta = 2(n_I + n_F)\omega_r$. For sufficiently long interaction times, terms proportional to $e^{i4(\pm 2j \pm 1)t}$ for $|j| \gg n$ oscillate rapidly and may be taken to be zero. We can then choose cutoffs $n_+ > \max(n_I, n_F)$ and $-n_- < \min(n_I, n_F)$ so that (9) reduces to a finite system which can be solved numerically. Figure 3 shows the relevant momentum states of an atom and laser fields for Bragg diffraction, transferring atoms from $|g, 0\hbar k\rangle$ to $|g, 6\hbar k\rangle$. The detuning of the undesired $2m$ -photon process $|g, 0, \hbar k\rangle \rightarrow |g, 2m\hbar k\rangle$ is $2m\delta - 4m^2\omega_r$. For the undesired intermediate states (solid blue, $m \neq n$) to remain unpopulated, δ_m for $m \neq n$ must be much greater than $\bar{\Omega}$. In practice, efficient transfers are determined by a number of factors including the time-dependence of the two-photon Rabi frequency, pulse width, shape, and the momentum spread of the atoms. A detailed discussion of these parameters in [21] is beyond the scope of this paper, but it is important to mention the last point regarding moving atoms. Our discussion so far has been confined to the case where the atoms are at rest relative to the standing wave ($\delta = 0$) caused by the Bragg beams. When $g_0(t)$ has some velocity Δv , then the ansatz (8) is modified, and the system of coupled differential equations becomes

$$i\dot{g}_n = \frac{\bar{\Omega}}{2} \left[g_{n+1} e^{i2(\delta - 2\omega_r \Delta v/v_r)t} e^{-i4(2n+1)\omega_r t} \right] + \frac{\bar{\Omega}}{2} g_{n-1} e^{-i2(\delta - 2\omega_r \Delta v/v_r)t} e^{i4(2n-1)\omega_r t},$$

where $v_r = \hbar k/m$ is the recoil velocity. In this case atoms with net velocity Δv are out of resonance with the Bragg condition $\delta = 2(n_F + n_I)\omega_r$ by $2\omega_r \Delta v/v_r$, but still only couple to higher or lower momentum states by multiples of $2\hbar k$. This is important since atoms for real interferometers always have some finite velocity distribution.

IV. OBSERVATION OF A GRAVITATIONAL AHARONOV-BOHM EFFECT

Several experimental verifications of the Aharonov-Bohm effect and the existence of the Berry phase have been realized since their theoretical conceptions ([7], [22]). However, these experiments, which were conducted around the 1980s-1990s, have exclusively been in the electromagnetic domain and used electrons and neutrons rather than neutral atoms as matter-wave sources. Analogous measurements for the much weaker gravitational analog have only been possible since around 2010 due to recent advances in light-pulse atom interferometers and

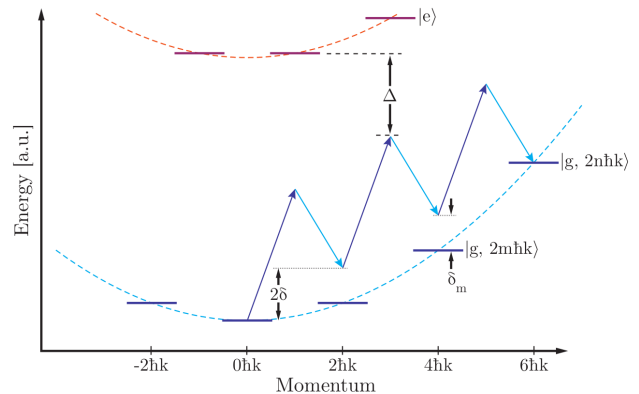


FIG. 3. Relevant momentum states of an atom and laser fields for Bragg diffraction. 2δ is the detuning between counter-propagating Bragg beams. Δ is the single-photon detuning of the lasers from $|e\rangle$. δ_m is the multi-photon detuning to an arbitrary intermediate ground state $|g, m\hbar k\rangle$. From [21].

growing interests in their role as ultraprecise quantum sensors [17], for which a notable example is the measurement of the gravitational acceleration to $3 \times 10^{-8}g$ by M. Kasevich and S. Chu [19].

In 2018, H. Müller and colleagues proposed an experiment for measuring the gravitational analog of the Aharonov-Bohm effect [23]. The setup consists of two identical spheres whose combined gravitational potential has a saddle point between the spheres x_A and two other points $\pm x_B$ near the spheres' centers. Atoms of mass m in the two arms of a Mach-Zehnder interferometer are moved to the two saddle points x_A, x_B by a moving optical lattice and spend a sufficiently long time $T = t_2 - t_1$ there, during which they accumulate phase shifts ϕ_A, ϕ_B . When the states are interfered at t_3 , the phase difference $\Delta\phi = \phi_A - \phi_B$ is measured by detecting the population in the outputs of the interferometer, which is given by $\cos^2 \Delta\phi/2$. The contribution to $\Delta\phi$ due to the gravitational Aharonov-Bohm effect, $\delta\phi_G$, is given by $m\Delta UT/\hbar$, where ΔU is the potential difference between x_A and x_B . While plausible, this proposal has not been realized since perturbations in the optical lattice required to transporting and suspending the atoms in the Earth's gravitational field would contaminate the interference signal [24].

A. Observation of the gravitational Aharonov-Bohm effect

In their recent work [4], Overstreet *et al.* used an atom interferometer in a "fountain" configuration, as shown in Figure 4, which does not require an optical lattice for suspending atoms during phase accumulation stage. A

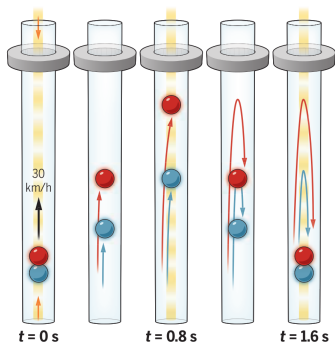


FIG. 4. A fountain atom interferometer. ^{87}Rb atoms are launched vertically from the bottom of a 10-meter vacuum tube and follow a free-fall trajectory. Laser pulses were applied at three different times to split, redirect, and recombine the wavepackets. The gravitational influence of the ring mass on the upper interferometer arm is measured from the interference signal. From [24].

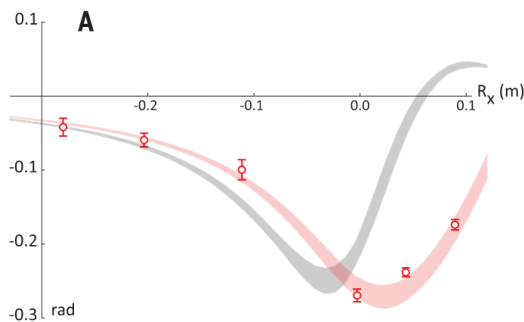


FIG. 5. Plot of the phase shift induced by the tungsten mass as a function of R_x . The red and gray curves are theoretical predictions. From [4].

simplified⁹ description of their experiment is as follows: ^{87}Rb atoms at $1\mu\text{K}$ are launched into a 10-m vacuum tube by an optical lattice. The matter-wave beamsplitters and mirrors transfer momentum to the atoms via Bragg diffraction, the process described in Section III C.

Here, the Bragg beamsplitter pulse transfers large momenta ($52\hbar k$) and wavepacket separation (25 cm), enhancing the sensitivity to the effect of the tungsten source mass at the top of the tube. The atoms receiving the $52\hbar k$ momentum kick travel upwards to a distance R_x from the tungsten mass. Finally, a mirror pulse followed by a beamsplitter pulse redirect and recombine the atoms and allow them to interfere. The atoms are then imaged by resonant scattering, and the interference pattern is observed. The measured phase shifts are in good agreement with ab-initio quantum mechanical calculations (see Figure 5).

V. CONCLUSIONS

In this paper, we re-introduce the notion of the Berry phase and interpret the Aharonov-Bohm effect as an example. Mirroring the role of matter-wave interferometers in the experimental verification of the magnetic Aharonov-Bohm effect, light-pulse atom interferometers have recently successfully detected the much weaker gravitational analog of this effect. In our brief introduction to atom interferometry, we review two atom-light interactions, namely stimulated Raman transitions and Bragg diffraction, which are the key ingredients to the workings of a modern light-pulse atom interferometer. The field of atom interferometry is incredibly rich with theory and experimental techniques that are vastly beyond the scope of this paper. However, the author hopes that this paper can serve as a good starting point for those interested in the subject.

ACKNOWLEDGMENTS

The author would like to thank Professor Zwierlein for his exciting AMO I lectures. 8.421 is the first *official* course in atomic physics for the author, and he looks forward to continuing his studies in 8.422: AMO II.

-
- [1] R. Shankar, *Principles of quantum mechanics* (Springer Science & Business Media, 2012).
 - [2] D. J. Griffiths and D. F. Schroeter, *Introduction to quantum mechanics* (Cambridge university press, 2018).
 - [3] J. J. Sakurai and E. D. Commins, “Modern quantum mechanics, revised edition,” (1995).

- [4] C. Overstreet, P. Asenbaum, J. Curti, M. Kim, and M. A. Kasevich, *Science* **375**, 226 (2022).
- [5] Y. Aharonov and D. Bohm, *Physical Review* **115**, 485 (1959).
- [6] W. Ehrenberg and R. E. Siday, *Proceedings of the Physical Society. Section B* **62**, 8 (1949).
- [7] A. Tonomura, N. Osakabe, T. Matsuda, T. Kawasaki, J. Endo, S. Yano, and H. Yamada, *Physical Review Letters* **56**, 792 (1986).
- [8] R. Chambers, *Physical Review Letters* **5**, 3 (1960).
- [9] H. Fowler, L. Marton, J. A. Simpson, and J. Suddeth, *Journal of Applied Physics* **32**, 1153 (1961).
- [10] P. Bocchieri and A. Loinger, *Il Nuovo Cimento A* (1965-1970) **47**, 475 (1978).

⁹ In the experiment, two interferometers are used, with one serving as a reference for removing contributions to the phase shift due to phase fluctuations in the laser fields. The interferometer also has components to account for deflections in the atom trajectories due to gravitational effects.

- [11] S. Roy, Physical Review Letters **44**, 111 (1980).
- [12] D. W. Keith, C. R. Ekstrom, Q. A. Turchette, and D. E. Pritchard, Physical Review Letters **66**, 2693 (1991).
- [13] O. Carnal and J. Mlynek, Physical Review Letters **66**, 2689 (1991).
- [14] H. Mueller, Atom Interferometry, Proceedings of the International School of Physics “Enrico Fermi” **188**, 339 (2014).
- [15] S. Dimopoulos, P. W. Graham, J. M. Hogan, M. A. Kasevich, and S. Rajendran, Physics Letters B **678**, 37 (2009).
- [16] B. Stray, A. Lamb, A. Kaushik, J. Vovrosh, A. Rodgers, J. Winch, F. Hayati, D. Boddice, A. Stabrawa, A. Niggelbaum, *et al.*, Nature **602**, 590 (2022).
- [17] K. Bongs, M. Holynski, J. Vovrosh, P. Bouyer, G. Condon, E. Rasel, C. Schubert, W. P. Schleich, and A. Roura, Nature Reviews Physics **1**, 731 (2019).
- [18] E. M. Rasel, M. K. Oberthaler, H. Batelaan, J. Schmiedmayer, and A. Zeilinger, Physical Review Letters **75**, 2633 (1995).
- [19] M. Kasevich and S. Chu, Applied Physics B **54**, 321 (1992).
- [20] E. Brion, L. H. Pedersen, and K. Mølmer, Journal of Physics A: Mathematical and Theoretical **40**, 1033 (2007).
- [21] B. V. Estey, *Precision Measurement in Atom Interferometry Using Bragg Diffraction*, Ph.D. thesis, UC Berkeley (2016).
- [22] A. Cimmino, G. Opat, A. Klein, H. Kaiser, S. Werner, M. Arif, and R. Clothier, Physical Review Letters **63**, 380 (1989).
- [23] M. A. Hohensee, B. Estey, P. Hamilton, A. Zeilinger, and H. Müller, Physical Review Letters **108**, 230404 (2012).
- [24] A. Roura, Science **375**, 142 (2022).